ELSEVIER

PII: S0266-3538(96)00088-7

Composites Science and Technology 56 (1996) 1283–1290

0266-3538/96/$15.00

EXPERIMENTAL MONITORING OF STRAIN LOCALIZATION AND FAILURE BEHAVIOUR OF COMPOSITE MATERIALS

M. G. D. Geers,[ab] T. Peijs,[a]* W. A. M. Brekelmans[a] & R. de Borst[ac]

[a]*Faculty of Mechanical Engineering, Eindhoven University of Technology, PO Box 513, Eindhoven, The Netherlands*
[b]*Faculty of Civil Engineering, Royal Military Academy, Brussels, Belgium*
[c]*Faculty of Civil Engineering, Delft University of Technology, Delft, The Netherlands*

(Received 9 February 1996; revised 6 June 1996; accepted 13 June 1996)

Abstract

Strain localization and failure behaviour of short-glass-fibre-reinforced polypropylene (SGFPP) have been investigated in compact tension (CT) specimens by using the Hentschel random access tracking system. The displacement fields measured in a zone behind the notch of the specimen are used to compute the strain fields during the entire loading process. From these strain fields process zones have been determined. Analysis of the results leads to an improved insight into the local failure behaviour of SGFPP and provides local and global experimental data for parameter estimation in numerical models. © 1996 Elsevier Science Limited

Keywords: Hentschel, compact tension, glass-fibre-reinforced polypropylene, strain localization, damage, process zone

1 INTRODUCTION

The analysis of strain localization and damage evolution in materials requires appropriate experimental techniques to verify the complex material behaviour in the damage zone. The mathematical description of damage and the localization process requires higher-order continuum models, e.g. non-local or gradient-dependent models.[1] These approaches remedy the deficiencies of the classical boundary value problem and can represent the physical failure process properly. In all these complex constitutive models a material parameter is introduced that has the dimension of length, and which is related to the dimensions of the localization zone.

The experimental problem now resides in the determination of this characteristic length. It cannot be measured in simple tests, since it depends intrinsically on the local deformation behaviour of the material. Therefore, a non-uniform test is required that triggers inhomogeneous deformations. In this experiment accurate local measurements have to be made in the localization zone. Experimental techniques that can measure locally are often based on optical methods, such as electronic speckle-pattern interferometry (ESPI),[2,3] Moiré interferometry [4,5] and the Hentschel random access tracking system.[6] Alternatively, length transducers or magnetic resonance imaging can be used, e.g. for the measurement of strain fields in the walls of the heart.[7] These methods provide information on the displacements at discrete points at the surface of the body, and are therefore well-suited for relatively thin structures. By using a gradient-deformation method,[8] strains can be computed accurately from the displacements, which is required in many theoretical models, including continuum damage mechanics (CDM) for the determination of threshold levels of damage.

The experimental monitoring of failure and damage phenomena in composite materials is an innovative research area, attracting more and more attention through an increasing interest in the failure behaviour of these materials. Interesting experiments have been carried out by Karger-Kocsis and Czigány[9–13] and Krey *et al.*[14] In these experiments mainly two techniques, namely acoustic emission (AE) and light microscopy (LM), were used to register the failure events in a fibre-reinforced composite material. Although qualitatively useful from a physical point of view, these experimental results do not provide any quantitative information on the local strains in the composite, and are therefore not well suited for a comparison with numerical simulations in which a length scale parameter has to be determined.

This study focuses on an experimental technique which provides local strain fields and which reveals the process zone, where damage is accumulated. It provides data which can be used to fit numerical simulations to the physical reality. Throughout the study, the experimental results are physically interpreted, using some physical and experimental

* To whom correspondence should be addressed.

observations by other authors[9–14] and the physical observation of the experiment itself. The Hentschel random access tracking system[6] is used to measure displacements locally in the failure zone of short-glass-fibre-reinforced polypropylene. Along with the registration of the local deformations, global force/displacement curves are obtained in a classical way.

2 EXPERIMENTAL

2.1 The compact tension test

The standard compact tension test (CT test) is a well-known standard test method for plane fracture of metals and for the measurement of fatigue crack growth rates. In this test the configuration is non-uniform, characterized by the presence of high deformation gradients in front of the notch of the specimen. The test, described in the ASTM Standard E399[15] and E647,[16] was adapted to the particular requirements imposed by composite materials.[17] The proposed testing protocol takes into account the major problems and difficulties in composites and polymers. The specimen is fixed at both the top and the bottom by a clevis and pin assembly. The specimen and loading arrangement is used for tension loading only.

The principal parameters that identify a CT specimen are the characteristic dimension W and the notch depth a (Fig. 1). The origin of the x-axis used in the experimental results has been chosen at the edge of the specimen. The CT specimens used in the current experiments were mechanically cut from SGFPP plates (Azdel® PD3243) with a thickness of 3·8 mm, kindly provided by GE Plastics Europe. The characteristic dimension W of the specimen used in the present study is 50 mm, since this size of specimen does not suffer from out-of-plane deformations. Other specimen sizes were tested for various loading conditions in a previous analysis.[18] The glass-fibre content of the SGFPP plates was 30 wt%, with a fibre length of 12·5 mm randomly distributed in the matrix. Different test conditions were applied by using different loading rates for each specimen size. Measurements were performed both dynamically (continuous increase of the deformations) and statically (step-wise increase of the deformations).

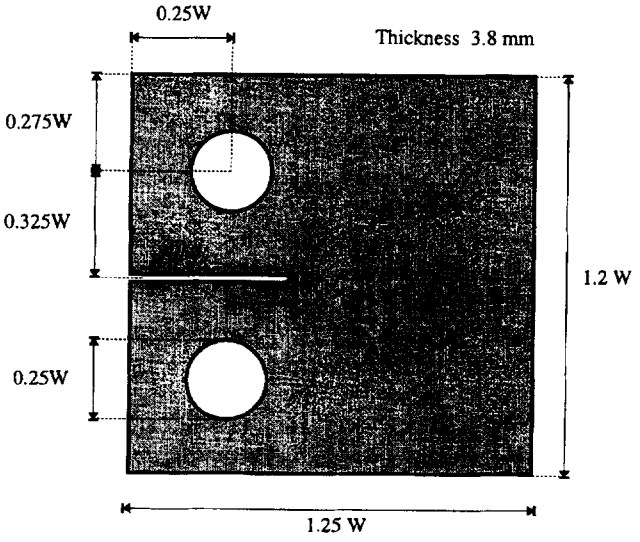

Fig. 1. The compact tension specimen.

2.2 Optical tracking of deformations in a CT specimen

The enhanced random access tracking system from Hentschel is based on a digital registration of optical signals from retro-reflective markers which are scanned by a random-access camera with image dissector.[6] The system, represented schematically in Fig. 2, tracks the positions of multiple points in space at high speed with a high resolution in real-time mode (real-time, high-speed, high-resolution, multi-point tracking). The sample rate can be speeded up to 7500 markers per second. The markers, made of a special retro-reflective foil, are illuminated by halogen light and are scanned by a high-speed window method. Each marker is traced in line-search mode within a small window around the centre of the marker. Inside this window the scanning is done by a sine-wave signal with a frequency of 120 kHz. These signals are transmitted from the camera to the video interface for further analysis and are transferred on-line to the computer which is connected to the system via a DMA interface. This on-line transfer is made possible by the window scan technique, necessitating only a small amount of data to be transferred. The parameters of the system can be adapted to the needs of a particular experiment by modifying the sample rate, the data transfer rate, and the number and the dimensions of the windows. The system offers a maximum resolution of 32678 by 32678 pixels within the field of view (f.o.v.). The smallest dimension of this field measures 30 mm by 30 mm in the experiments that have been performed. The size of the trace windows around the markers can be adapted discretely from 0·5 to 4% (f.o.v.). The effective resolution is reduced when the window size increases because of a limited window resolution of 256 by 256 pixels.

The video interface is designed to operate and control simultaneously two cameras, thus offering a full stereoscopic displacement set. Combining data from both cameras gives the deformation of each marker in a three-dimensional space. Only one camera is used for the in-plane analysis of CT specimens. The accuracy that can be achieved with this dynamic measurement system is better than 0·1% of the f.o.v., if calibration and distortion correction are adequately performed. For the CT specimen used in the present study this accuracy equals approximately 30 μm.

The accuracy of all measurements is enhanced by an

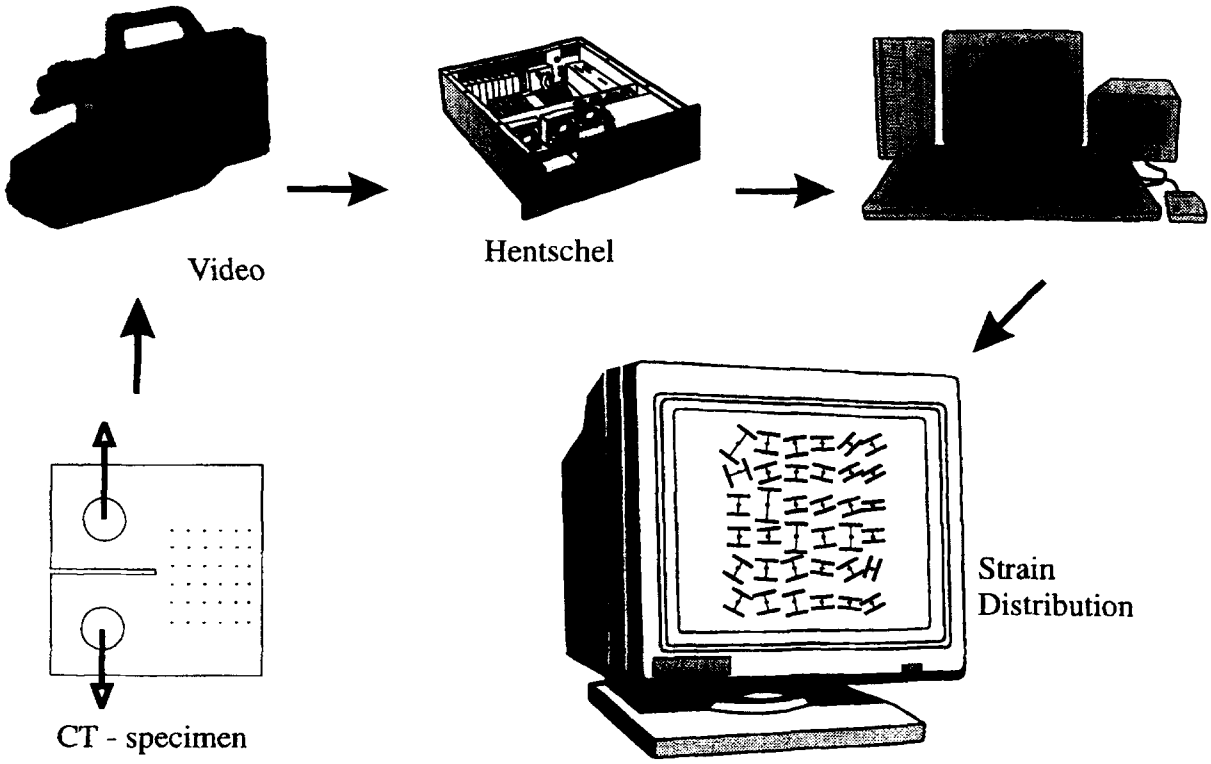

Fig. 2. Experimental set-up for the Hentschel strain measurement system.

appropriate filtering scheme. Several mathematical techniques exist to reduce the effect of noise, such as digital filtering, Chebyshev polynomial or spline fitting, or the use of Fourier analysis applied to multidimensional data. These methods smooth the data in time and do not take advantage of the known mechanism that generates the data. Herein, the singular value decomposition (SVD) filtering scheme[19] is used, which takes into account the mutual relationship between the marker displacements sharing a common continuum. By the use of this filtering technique on the raw data matrix, the noise free marker coordinate matrix is estimated in a least-squares sense.[20,21].

An initial precise static measurement of the undeformed state is used as the reference state in all strain computations. Furthermore, the results obtained from the static measurements are statistically corrected by taking multiple samples of the static deformation field.

3 LOCAL DEFORMATION BEHAVIOUR OF SGFPP

3.1 Strain fields and failure mechanisms

The dynamic and static CT tests that have been performed have resulted in a set of displacement fields with their corresponding strain fields computed by a gradient-deformation formulation[8] applied to the filtered displacements. The results obtained from these computations can be visualized graphically at different loading steps. Most of these tests gave reliable and reproducible results, which makes it possible to limit the analysis to the representative data reflecting the common conclusions of all tests. Figure 3 gives a three-dimensional view of the y component of the strain (in the load direction) in the CT specimen. The computed strain field is depicted over the entire marker field of the elastically deformed CT specimen (initial loading phase). The small elastic deformations in the composite specimen are retrieved within an accuracy of 0·1%. The localization zone behind the notch is located within the process zone where damage is being built up. Noise reduction is done efficiently, yielding a smooth continuous strain field.

During the entire loading process, strains have also been computed over the crack that splits the specimen progressively. The strains derived from these displacements over the crack region will be denoted as fictive strains. The use of such fictive strains can be justified in continuum damage mechanics, where the cracks are treated continuously as fully damaged material. The numerical values computed for these fictive strains may be large, and can exceed 100% in the final failure stage. In the continuous strain field of the continuum, a threshold value exists beyond which the computed strain can no longer be considered as a measure of

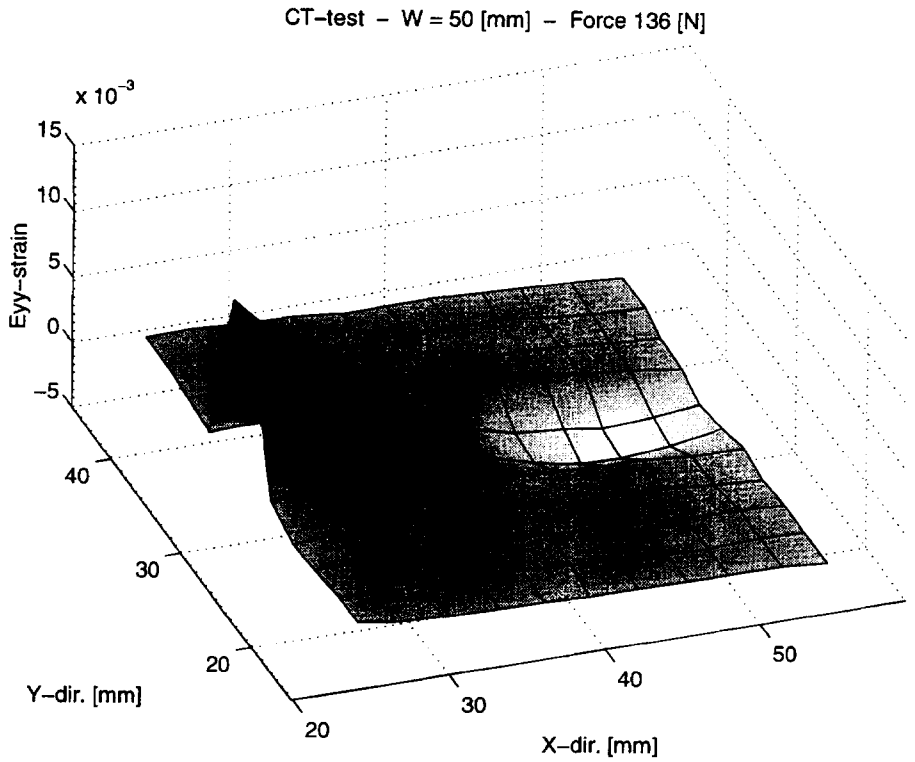

Fig. 3. ϵ_{yy} strain field measured on the marker grid.

material elongation. The fictive strains exceeding this threshold value are essential characteristics of a physical crack (crack opening and propagation), along with the associated displacements. An essential difficulty in modelling composites behaviour is the fibre bridging in the crack zone. There is no physical threshold value which can take this fibre bridging into account. It is therefore necessary to take an appropriate threshold value that represents the entire process zone and a part of the crack zone where fibre bridging occurs (see Section 3.1.1).

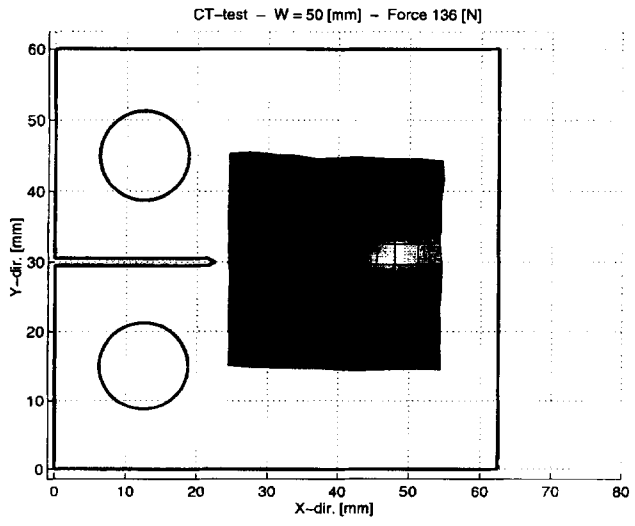

Fig. 4. ϵ_{yy} strain field.

The initial elastic region covers an important fraction of the marker field. The extent of this region changes significantly during the test, and reveals important characteristics with respect to the failure behaviour of SGFPP. A projected plane greyscaled view of the elastic strain field (Fig. 4) illustrates the affected area where strains localize. Figure 4 also shows the spatial location of the markers on the CT specimen (grid points), by embedding the entire strain field in its CT configuration.

The entire deformation process can be monitored by sampling the strain field during the loading process. The characteristic force/displacement curve (FD curve) is shown in Fig. 5. During the deformation process 34 samples have been taken. Four of these samples are marked on the FD graph. Two samples were taken before the maximum force was reached, whereas the other two samples were taken after this maximum. The corresponding strain fields (the y strain component) are depicted in Fig. 6, where the fictive strain reaches a maximum value of 30%. These strain fields clearly show the changes in size and amplitude of the compressive zones in the CT specimen during the loading process.

The steep ascending branch of the FD curve results mainly from the local build-up of the elastic strains and partially from the irreversible crack initiation. The

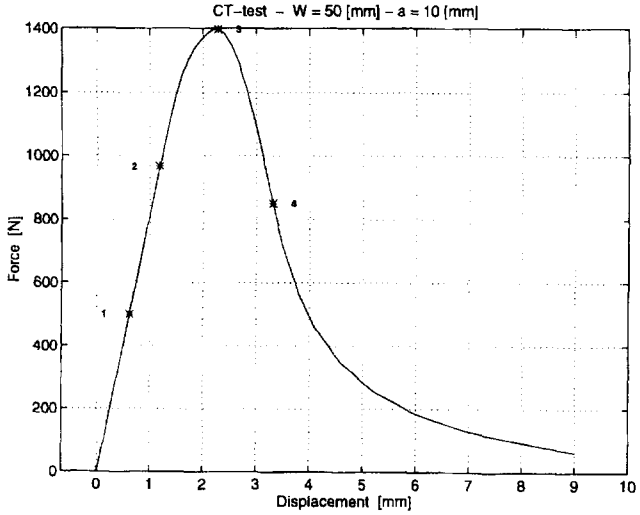

Fig. 5. Force/displacement curve.

strain in the zone of measurement reaches a maximum value of approximately 10%, at which the material may be considered as fully damaged. The ultimate strain that can be reached in classical tensile tests on SGFPP, is approximately 3%. This tensile strain of 3% evidently underestimates the actual strains in the localization zone. One of the main reasons that underly the differences between tensile tests and CT tests is the nature of the failure mechanism. This mechanism consists of a sequence of matrix deformation, matrix cracking, fibre/matrix debonding and fibre pull-out. The fibre/matrix debonding and fibre pull-out are two mechanisms characterized by significant displacements and thus by high strains. In a CT test damage and failure develops progressively through the specimen. In a tensile test, the large elastically deformed zone releases the deformation energy almost instantaneously at failure. The unstable fibre/matrix debonding and fibre pull-out which occur in this short period can therefore not be taken into account for the measurement of the maximum strain. It should be noted that, after the test, the two parts of the specimen are not fully separated since the fibre pull-out is not yet completed. In the CT test for this particular material, the mechanisms of fibre/matrix debonding and fibre pull-out are initiated before the maximum load is achieved.

3.1.1 The process zone

In order to locate the process zone in the strain field, the strain computations and representations have been slightly modified. The fictive strains which characterize highly cracked material are ignored, as displacements over this crack region are no longer taken into account to compute the associated strain fields. An appropriate threshold value of 5% for the strains has been used to locate the crack opening zone. This threshold value exceeds the strain limit for crack initiation determined at the end of this paragraph and will therefore enclose the entire process zone and a part of the crack zone where fibre bridging is significant. Using this threshold value, attention will be mainly focused on the qualitative evolution of the process zone. Furthermore, a graphical representation is given in Fig. 7 in which the very small elastic strains in the specimen and the negative strains in the compressive zone are left out of consideration. The image thus found only reflects the zone where positive high strains occur, leading to damage and failure behind and at the crack tip.

Using the same samples as depicted in Fig. 5, a dynamic evolution of the process zone can be obtained (Fig. 8). The process zone moves to the interior of the specimen as the crack propagates. Strikingly, the changes in size of the process zone

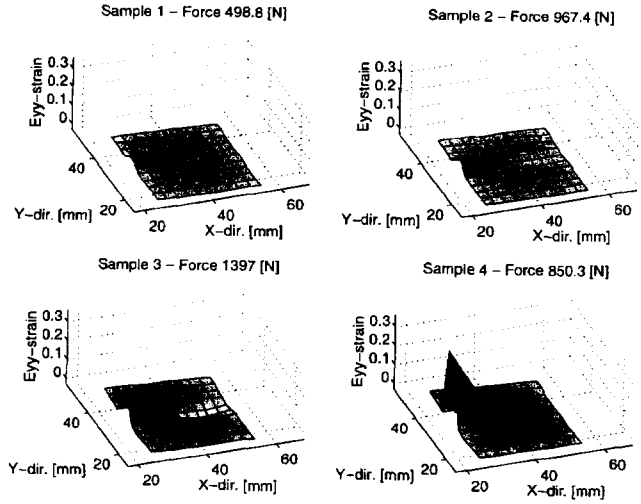

Fig. 6. ϵ_{yy} strain field evolution in a CT specimen ($W = 50$ mm).

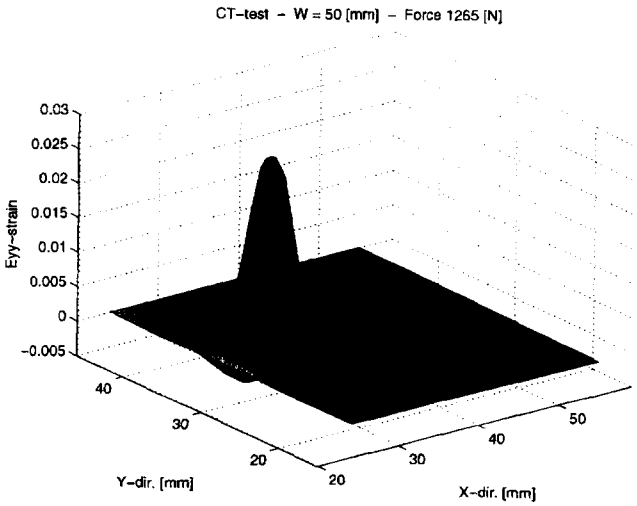

Fig. 7. Process zone behind crack tip.

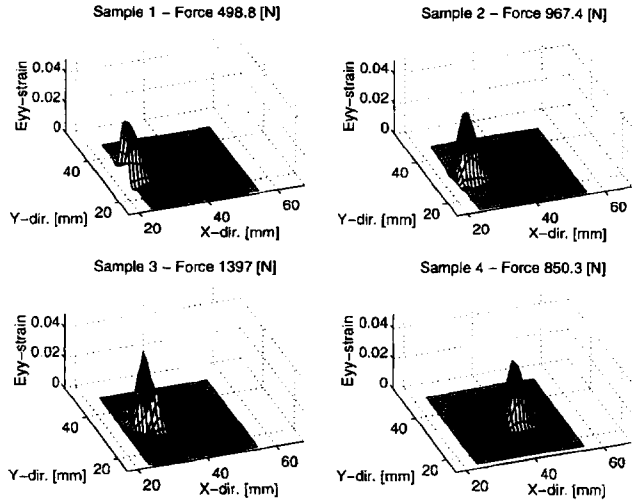

Fig. 8. Propagation of the process zone.

remain very limited during this evolution. This is shown more clearly by plotting contour lines, which show the area of the CT specimen where a strain level of, for instance, 2·2% is exceeded. Six of the 34 available samples have been plotted in Fig. 9. Again, the shift of the fracture process zone into the interior of the CT specimen is clear. The changes in shape are mainly affected by single markers just exceeding the threshold of 2·2%.

Additionally, attention is focused on the variation of the equivalent strain in the specimen. The equivalent strain here is defined as:

$$\epsilon_{eq} = \sqrt{\epsilon_{xx}^2 + \epsilon_{yy}^2 + 2\epsilon_{xy}^2}$$

In continuum damage mechanics an equivalent strain is often used as a measure for the internal damage variable. Note that the differences between this equivalent strain and the strain component aligned with the load line (ϵ_{yy}) are minor in this particular test. The distribution of the equivalent strain with respect to different strain levels evolves as shown in Fig. 10. This figure represents all 34 samples taken during the experiment.

Figure 10 shows that the percentage of observations in the 2–3% range grows rapidly to a maximum value, and then starts to decrease shortly after the ultimate load has been reached (Fig. 5). During the initiation of failure, a large elastically deformed zone is built up, which starts to decrease when fibre/matrix debonding occurs. When a displacement of 2 mm is reached a part of the material starts to unload, since the percentage of observations in the 2–3% zone decreases in favour of the observations in the 0–2% zone and in the 3–4% zone. This phase mainly controls the crack initiation and propagation through the specimen, and is attended by a release of the accumulated elastic energy. After a displacement of 4 mm the number of observations exceeding the strain level of 4% stabilizes. Crack propagation is slowed down, and all further deformations are mainly caused by crack opening.

Another interesting observation can be made regarding the limit value, which characterizes the presence of an irreversible crack in the composite material. It can be read from Fig. 10 that the zone with strains above 4% never reduces, implying that the initiation value for cracking and fibre pull-out is smaller than 4%. It can also be noticed that this is not the case for the 3–4% zone. This unknown strain limit must therefore reside between 3% and 4%. A more sensitive computation was carried out, to retrieve a better prediction of this strain limit. The strain value, above which the affected zone does not experience a size reduction, has been computed. A mean value of

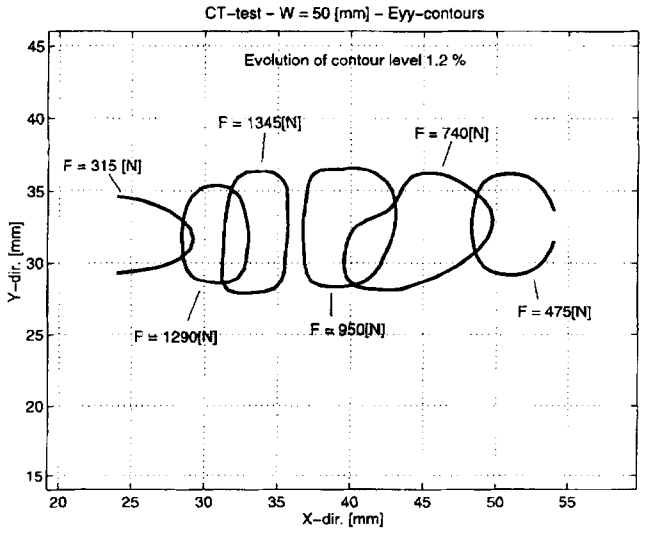

Fig. 9. Contour lines delimiting the process zone.

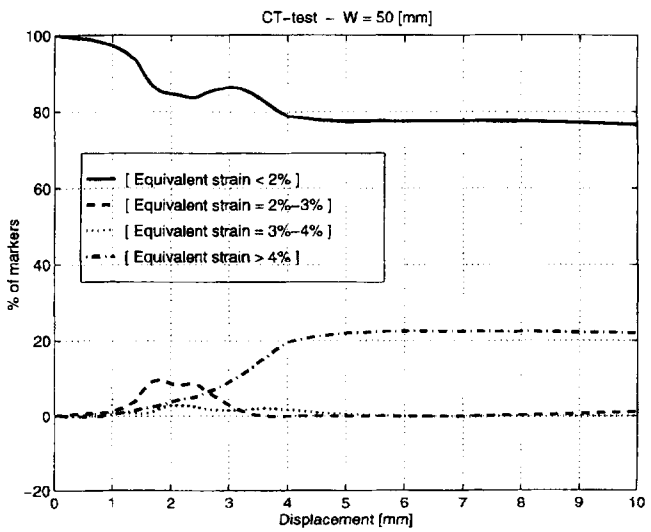

Fig. 10. Distribution of the equivalent strains.

3·5% with a standard deviation of 0·3% was found when all tests were considered.

4 CONCLUSIONS

The numerical results from the present experiments can be well understood if they are compared to some physical observations which have been carried out for SGFPP and other composite materials.[9–14] The deformation and failure process of SGFPP in a CT test consists of the following phases:

- Build-up of a wide elastically deformed zone behind the notch tip. This process is mainly controlled by matrix deformation.
- Crack initiation above a threshold value for the equivalent strain (exceeding 3%). Matrix deformation and fibre/matrix debonding characterize this stage.
- The load reaches the maximum value and decreases subsequently. Unloading of the elastically deformed zone accompanied by crack propagation. Fibre/matrix debonding and some fibre pull-out.
- Stabilization of the crack propagation, crack opening.

The damage process zone behind the crack tip mainly covers the elastic deformation and the crack initiation mentioned above. These different deformation stages can be identified in all tests, for all sizes and all loading rates. The present conclusions regarding the fracture behaviour and the failure modes of SGFPP in the CT test are in agreement with those following from the AE and LM techniques,[9–14] and additional details with respect to the failure process are retrieved.

The non-uniform compact tension tests that were performed provide global (force/displacement) and local (displacement fields and strain fields) data which are of great use in fitting procedures for estimating the parameters of a constitutive model or the length scale in higher-order continuum descriptions. Classically, most fitting procedures are limited to global results. In the particular case of short-glass-fibre-reinforced polypropylene, the present local CT results permit evaluation of numerical models and give indications on the adaptation of those numerical models that might fit the physical reality globally but not locally.

REFERENCES

1. de Borst, R., Sluys, L. J., Mühlhaus, H.-B. & Pamin, J., Fundamental issues in finite element analysis of localisation of deformation. *Engng Comput.* , **10** (1993) 99–122.
2. Bergmann, D., Galanulis, K., Ritter, R. & Winter, D., Application of optical field methods in material testing and quality control, electronic speckle pattern interferometry and grating method. In *Photomécanique* 95, Edition Eyrolles, 1995, pp. 257–265.
3. Galanulis, K. & Ritter, R., Speckle interferometry in material testing and in dimensioning of structures. In *SPIE*, Vol. 2004, *Interferometry VI: Applications*, 1993, pp. 269–275.
4. Post, D., Han, B. & Ifju, P. G., *High Sensitivity Moiré, Experimental Analysis for Mechanics and Materials*. Springer, New York, 1994.
5. Han, J. H. & Mao, T. X., The application of Moiré interferometry in the measurement of displacement field and strain field at notch-tip and crack-tip. *Acta Mech. Sin.*, **7** (1991) 376–382.
6. Zamzow, H., The Hentschel random access tracking system hsg 84.30. *SPIE*, **1356** (1990) 130–133.
7. Hunter & Zerhouni, E. A., Imaging distinct points in left ventricular myocardium to study regional wall deformation. In *Innovations in Diagnostic Radiology*, ed. J. H. Anderson. Springer, New York, 1989, pp. 169-190.
8. Geers, M. G. D., de Borst, R. & Brekelmans, W. A. M., Computing strain fields from discrete displacement fields in 2D-solids. *Int. J. Solids Struct.*, **33** (1996) 4293–4307.
9. Karger-Kocsis, J., Fracture mechanical characterization and damage zone development in glass fiber mat-reinforced thermoplastics. *Polym. Bull.*, **31** (1993) 235–241.
10. Karger-Kocsis, J. & Czigány, T., Fracture behaviour of glass-fibre mat-reinforced structural nylon rim composites studied by microscopic and acoustic emission techniques. *J. Mater. Sci.*, **28** (1993) 2438–2448.
11. Czigány, T. & Karger-Kocsis, J., Determination of the damage zone size in textile fabric reinforced polypropylene composites by locating the acoustic emission. *Polym. Polym. Compos.*, **15** (1993) 329–339.
12. Czigány, T. & Karger-Kocsis, J., Comparison of the failure mode in short and long glass fiber-reinforced injection-molded polypropylene composites by acoustic emission. *Polym. Bull.*, **31** (1993) 495–501.
13. Karger-Kocsis, J., Yuan, Q. & Czigány, T., Assignment of acoustic emission to the failure sequence and damage zone growth in glass fiber strand mat-reinforced structural nylon RIM composites. *Polym. Bull.*, **28** (1992) 717–723.
14. Krey, J., Friedich, K. & Schwalbe, K.-H., Fracture toughness and fatigue crack propagation of single fibre-bundled reinforced model composites. *J. Mater. Sci. Lett.*, **6** (1987) 851–856.
15. ASTM, ASTM E399-90, standard test method for plane-strain fracture toughness of metallic materials. In *Annual Book of ASTM Standards, Section* 3, *Metals Test Methods and Analytical Procedures*. American Society for Testing and Materials, 1993.
16. ASTM, ASTM E647-93, Standard test method for measurement of fatigue crack growth rates. In *Annual Book of ASTM Standards, Section* 3, *Metals Test Methods and Analytical Procedures*. American Society for Testing and Materials, 1993.
17. Williams, J. G. & Cawood, M. J., European Group on Fracture: K_c and G_c methods for polymers. *Polym. Testing*, **9** (1990) 15–26.
18. Geers, M. G. D., Peijs, T., de Borst, R. & Brekelmans, W. A. M., Experimental dynamic analysis of damage evolution in short fibre-reinforced composite materials. In *Proc. 10th Int. Conf. on Composite Materials, Fatigue and Fracture*, Vol. I, ed. A. Poursartip and K. Street, pp. 755–762.

19. Muijtens, A. M. M., Prinzen, J. M. A., Hasman, T. T., Reneman, A. & Arts, R. S., Noise reduction in estimating cardiac deformation from marker tracks. In *Special Communications*, American Physiological Society, 1990.
20. Deprettere, F. (ed.), *SVD and Signal Processing-algorithms, Applications and Architectures*. Elsevier Science–Delft University of Technology, Delft, The Netherlands, 1988.
21. Golub, G. H. & Van Loan, C. F., *Matrix Computations*. North Oxford Academic/Johns Hopkins University Press, 1983.